RAPID COMMUNICATIONS

PHYSICAL REVIEW A VOLUME 34, NUMBER 1 JULY 1986

Type-II intermittency in a periodically driven nonlinear oscillator

P. Richetti, F. Argoul, and A. Arneodo*

Centre de Recherche Paul Pascal, Université de Bordeaux I, Domaine Universitaire, 33405 Talence Cedex, France

(Received 16 December 1985)

We report on the first numerical observation of type-II Pomeau-Manneville intermittency in a periodically driven third-order nonlinear oscillator. A discussion of such a transition to chaos in terms of the interaction of a local instability (subcritical Hopf bifurcation) and a global instability (homoclinic bifurcation) of a periodic motion is provided. We investigate the distribution of the laminar lengths and compare our numerical results with the theory. Emphasis is given to the $1/f^{\delta}$ divergence ($\delta \sim 0.67 \pm 0.10$) observed in the small-frequency limit of power spectra.

Among the well established routes to deterministic chaos,[1-3] the so-called Pomeau-Manneville scenario[4] has received considerable interest, both in an experimental as well as in a theoretical context. This fascinating scenario is characterized by short irregular or turbulent bursts interrupting, seemingly at random, a nearly regular (periodic) signal. Such an intermittent transition to weak turbulence arises in the process of destabilization of a limit cycle. Three different types of intermittencies have been originally[4] distinguished according to the nature of the local bifurcation:[5-7] Type-I intermittency is associated with a saddle-node bifurcation (a real Floquet multiplier crosses the unit circle at $+1$), type-II intermittency comes with a subcritical Hopf bifurcation (two complex conjugate multipliers cross the unit circle), and type-III intermittency involves a subcritical period-doubling bifurcation (a real multiplier crosses the unit circle at -1). However, such a local instability is not the only ingredient required for intermittency to occur. The conjecture which accounts for intermittency is that simultaneously[8] to the local linear instability, there is a global nonlinear mechanism (strange attractorlike behavior) which ensures the dynamics to be reinjected in the neighborhood of the limit cycle. In (Ref. 4) this property was obtained in periodizing the phase space. In most of the theoretical studies[9] the reinjection process has been phenomenologically modeled by random reentries with white probability distribution. In numerical as well as real experiments one can reasonably expect to observe deviations from such a theoretical hypothesis.

Since the pioneering work of Manneville and Pomeau,[4] type-I intermittency has been frequently encountered in numerical studies of ordinary differential equations (ODE) and discrete dynamical systems.[9-11] Detailed measurements of type-I intermittency have been carried out with different experimental devices.[12-15] More recently, type-III intermittency was observed in Rayleigh-Benard convection in confined geometry.[16] But so far, there have been no examples identifying type-II intermittency in either real experiments or in simulation studies. The main purpose of this paper is not only to report about the discovery of type-II intermittency in a periodically driven nonlinear oscillator but also to discuss the strategy we have adopted to give evidence of such a scenario to chaos.

Consider the following ODE system:[17]

$$\dddot{X}+\eta\ddot{X}+\nu\dot{X}+\mu X+k_1X^2+k_2\dot{X}^2+k_3X\dot{X}+k_4X\ddot{X}+k_5X^2\ddot{X}=F\cos(\omega t)\ . \quad (1)$$

In the limit of vanishing amplitude of the periodic forcing ($F=0$), this system reduces to a third-order autonomous ODE, which has been shown to arise naturally as the truncated normal form of a triply degenerate problem[18] (the dispersion relation has a triple zero eigenvalue at the triple point $\eta=\nu=\mu=0$). Special interest was dedicated to the study of this amplitude equation which exhibits period doublings and strange attractorlike behavior as close as we want to the onset of the triple instability. The main step in our approach to type-II intermittency consists of showing that this truncated amplitude equation also accounts for the interaction of a subcritical Hopf bifurcation and a global homoclinic bifurcation.[5-7]

For $F=0$, Eq. (1) possesses two equilibria $X^*=0$ and $-\mu/k_1$. Both these equilibria display a Hopf bifurcation when $\mu=\eta\nu$ and $\mu=-\eta\nu$, respectively ($\eta,\nu>0$). From now on let us focus on the origin, keeping in mind that our argument extends to the nontrivial steady state. In the neighborhood of the critical surface $\mu=\eta\nu$, the use of both the center manifold theorem and the normal form techniques[5-7] allows us to reduce Eq. (1) to a two-dimensional system which can be conveniently written in polar coordinates as

$$\begin{aligned}\dot{\rho}&=\lambda\rho+a\rho^3+\text{higher-order terms}\ ,\\ \dot{\theta}&=\Omega+b\rho^2+\text{higher-order terms}\ ,\end{aligned} \quad (2)$$

where $\lambda\sim(\mu-\eta\nu)$ measures the distance to the critical surface and $\Omega=\sqrt{\nu}+O(\lambda)$. The coefficients a and b are computed on this surface. The detailed expressions of these coefficients in terms of the parameters k_i of the nonlinear terms in Eq. (1) are very complicated. Let us simply mention here that the arbitrariness in the choice of the k_i's recovers both the situations $a>0$ and $a<0$, which correspond to subcritical and supercritical Hopf bifurcations, respectively.

As discussed in Ref. 18, the strange attractorlike behavior displayed by Eq. (1), for $F=0$, can be interpreted in terms of chaotic orbits which occur in nearly homoclinic conditions as ensured by a theorem of Shil'nikov.[19] We did not ascertain analytical conditions for the existence of such homoclinic orbits, but we have located these conditions using a numerical technique elaborated on in Ref. 20. Thanks to a simple trial and error method we traced the homoclinic bifurcation up to a close neighborhood of the previously described subcritical Hopf bifurcation. In such research, the saturating highest-order term $k_5X^2\ddot{X}$ added in Eq. (1) has been of great help. Such a "concomitant" situation favors

the application of the Shil'nikov theorem: The homoclinic orbit is biasymptotic to a saddle focus, the origin, which satisfies the requirement[18,19] that the negative real root of the corresponding dispersion relation has larger magnitude than the real part [$\lambda \gtrsim 0$, in Eq. (2)] of the complex-conjugate roots. Hence, as already experienced in Ref. 20, there is hope that asymptotically stable chaotic motions will be observed within the conditions where the homoclinic orbit has been (numerically) shown to exist. Moreover, if anything, this chaotic behavior will ensure a reinjection of the dynamics in the neighborhood of the origin. We actually performed a numerical investigation of Eq. (1) without forcing, and for different values of the control parameter μ. As suspected theoretically, when varying μ through the subcritical Hopf bifurcation value, we do witness a direct transition from rest to a turbulent regime. This transition manifests itself as chaotic bursts, which from time to time emerge from a nearly stationary signal.

When turning on the periodic driving ($F \neq 0$), such a scenario to chaos generalizes to type-II intermittency. Figure 1 illustrates the results of a numerical investigation of Eq. (1) for the parameter values $F=0.5$, $\omega=15$, $\eta=1$, $\nu=1.2$, $k_1=-100$, $k_2=120$, $k_3=0$, $k_4=-20$, $k_5=100$. Three time series are represented corresponding to three different values of μ: (a) $\mu=1.14$: below the subcritical Hopf bifurcation we observe a periodic signal with a frequency equal to the driving frequency; (b) $\mu=1.16$: just above the subcritical Hopf bifurcation very exceptional short bursts of chaos interrupt very long laminar episodes; (c) $\mu=1.25$: far above criticality the chaotic episodes become more frequent; their average length increases with μ at the expense of the laminar phase duration. Enlargements of the time series in Fig. 1(c) are shown in Fig. 2. It is clear in these pictures that the occurrence of chaotic bursts comes with a modulation of the original periodic oscillation at the frequency $\Omega \sim \sqrt{\nu} \sim \frac{1}{13}$ in ω-units; the amplitude of this modulation increases slowly initially, but when it reaches a high value the increase becomes very rapid. Then the signal loses its regularity and a turbulent episode is initiated. Immediately after the chaotic intermission there is a reappearance of the regular behavior, corresponding to a return to

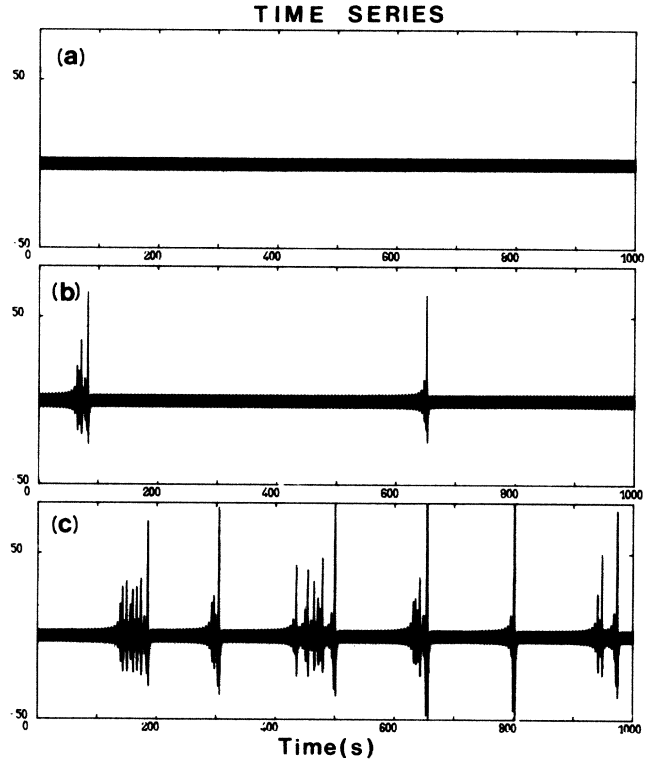

FIG. 1. Time plot of $\ddot{X}$ (unit scale $=10^{-2}$) as computed with Eq. (1) for (a) $\mu=1.14$, (b) 1.16, and (c) 1.25. The model parameter values are given in the main text.

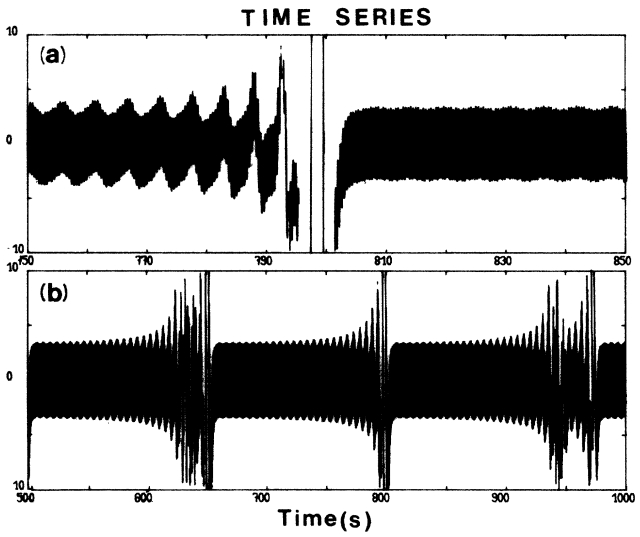

FIG. 2. Enlargements of the time series for $\mu=1.25$. (a) and (b) differ in the dilatation rate of the time scale.

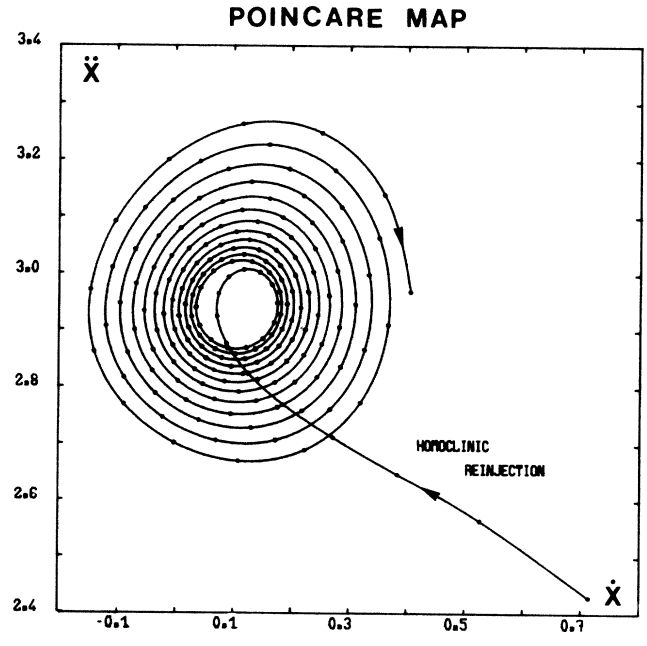

FIG. 3. A stroboscopic Poincaré map corresponding to the time series shown in Fig. 1(c). This picture represents an enlargement of this map in the neighborhood of the underlying saddle focus as projected onto the $(X\ddot{X})$ plane.

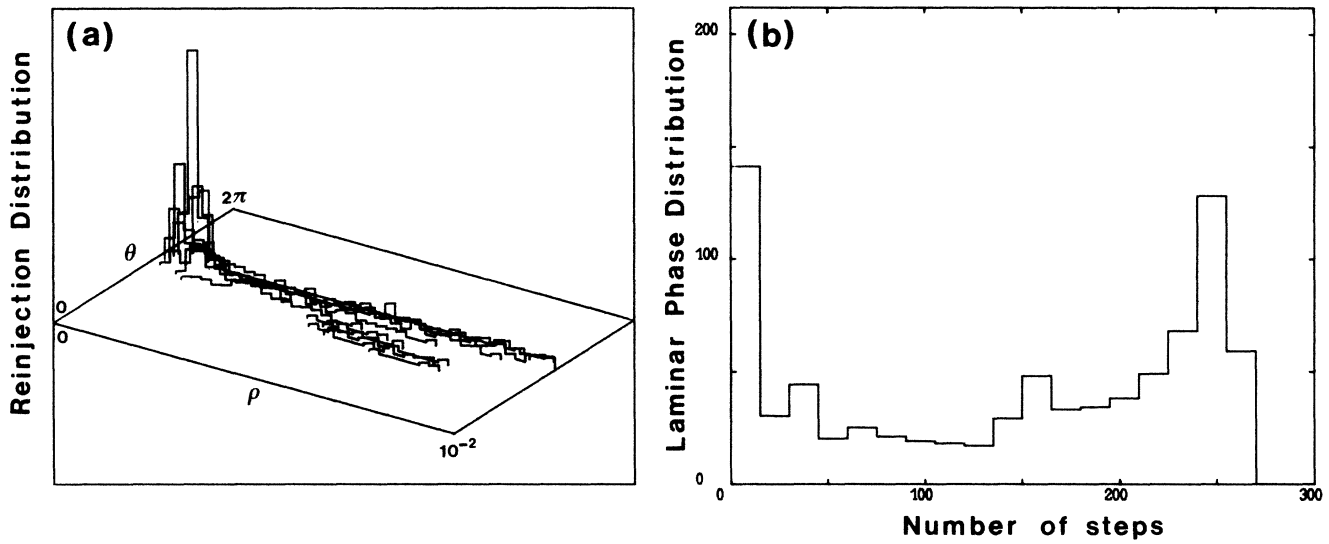

FIG. 4. (a) Reinjection distribution inside the two-dimensional unstable manifold of the fixed point $\rho = 0$ and (b) probability distribution $P(n)$ for the laminar lengths; same model parameters as in Fig. 1(c).

the preceding periodic behavior. The position of the reentry point determines the length of the following laminar period.

When dealing with systems like Eq. (1), where an external periodic forcing occurs, the usual way to define a Poincaré first return map consists of sampling the orbits in phase space at the frequency of the forcing. Figure 3 represents such a defined three-dimensional Poincare map as computed from the time series in Fig. 1(c). Only a few points have been retained in this figure in order to distinguish both the one-dimensional homoclinic reinjection process in the neighborhood of the fixed point and the very mild spiraling behavior away from this point which corresponds to a laminar phase.

Taking advantage of the rotational invariance of the Hopf normal form for mappings,[5-7]

$$\rho_{n+1} = (1+\epsilon)\rho_n + a\rho_n^3 + \text{higher-order terms} ,$$
$$\theta_{n+1} = \theta_n + \Omega + b\rho_n^2 + \text{higher-order terms } (\Omega \text{ irrational}) , \quad (3)$$

the theoreticians have assumed uniform reinjection distribution in a disk ($\rho <$ const) contained in the two-dimensional unstable manifold of the fixed point. Within such a working hypothesis, the probability distribution $P(n)$ of the laminar lengths is predicted to behave like $P(n) \sim n^{-2}$ at small laminar period n, and to decay exponentially $P(n) \sim \exp(-2\epsilon n)$ at large n.[4] In addition, the average length of the laminar episodes is expected to scale like $\langle n \rangle \sim \ln(1/\epsilon)$, where $\epsilon \sim \mu - \mu_I$ is characteristic of the distance from the intermittency threshold $\mu_I \sim 1.149 \ldots$.

The reinjection distribution corresponding to the time series in Fig. 1(c) is shown as the histogram in Fig. 4(a). The whole set of reentry points falls into a narrow range in the θ variable, clearly indicating that the homoclinic reinjection process not only breaks the rotational invariance of Eq. (3),[21] but that it is, in fact, intrinsically one dimensional. Therefore, one can expect to observe severe deviations from the theoretical predictions. The corresponding probability distribution of laminar length $P(n)$ is illustrated in Fig. 4(b). $P(n)$ appears to be peaked not only at low n values but also at high n values ($n \sim 250$), which at first sight is rather puzzling with respect to the predicted exponential decay. Indeed, such a peak simply reflects the particular shape of the reinjection distribution which [as seen in Fig. 4(a)] is peaked toward the small ρ values: All the reentry points fall almost on a curve, but with a high density in the neighborhood of the fixed point, which runs counter to the observation of an exponential tail in $P(n)$. The computation of $\langle n \rangle$ for values of μ ranging from 1.15–1.30 yields $\langle n \rangle \sim \epsilon^{-1/2}$, which contradicts the expected $\ln(1/\epsilon)$ behavior, but which is in fair agreement with the theoretical scaling relation derived when assuming a one-dimensional reinjection process.[4]

As emphasized in Refs. 22 and 23, the arbitrarily long laminar regions observed on an intermittent time series manifest as $1/f^{\delta}$ divergencies in the small-frequency limit of

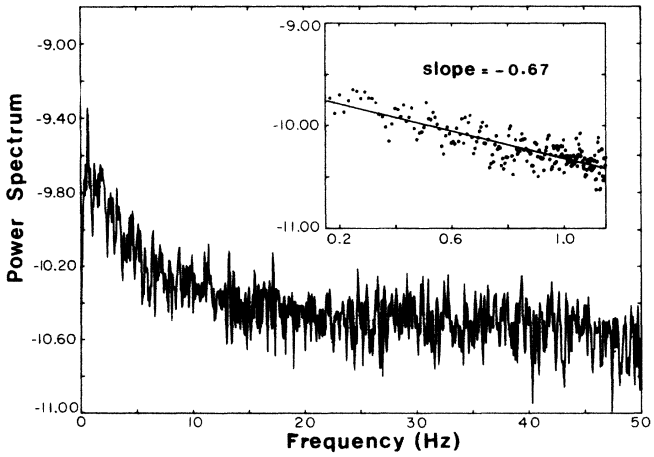

FIG. 5. Power spectrum as computed with Eq. (1) for $\mu = 1.15$. In the inset, the power spectrum is plotted vs $\ln f$.

power spectra. Figure 5 illustrates the power spectrum computed from the Poincaré map obtained at the value $\mu = 1.15$ immediately above the intermittency threshold. A low-frequency $1/f^{\delta}$ behavior is detected with $\delta \sim 0.67 \pm 0.10$. In the frequency range reported in Fig. 5, this numerical estimate of the exponent δ is quite compatible with the logarithmic corrections to a $1/f^{1/2}$ divergence as predicted when considering a one-dimensional reinjection mechanism.[23]

We are very grateful to R. Schumaker for a careful reading of the manuscript and the Centre National de la Recherche Scientifique for an ATP grant.

---

*Permanent address: Laboratoire de Physique Théorique, Université de Nice, Parc Valrose, 06034 Nice Cedex, France.

[1]J. P. Eckmann, Rev. Mod. Phys. **53**, 643 (1981).

[2]E. Ott, Rev. Mod. Phys. **53**, 655 (1981).

[3]N. B. Abraham, J. P. Gollub, and H. L. Swinney, Physica D **11**, 252 (1984), meeting report.

[4]P. Manneville and Y. Pomeau, Phys. Lett. **75A**, 1 (1979); Commun. Math. Phys. **74**, 189 (1980).

[5]V. I. Arnold, *Supplementary Chapters to the Theory of Ordinary Differential Equations* (Nauka, Moscow, 1978).

[6]G. Iooss, *Bifurcation of Maps and Applications* (North-Holland, Amsterdam, 1979); G. Iooss and D. D. Joseph, *Elementary Stability and Bifurcation Theory* (Springer, NY, 1980).

[7]J. Guckenheimer and P. Holmes, *Nonlinear Oscillations, Dynamical Systems, and Bifurcations of Vector Fields* (Springer, Berlin, 1984).

[8]C. Tresser, P. Coullet, and A. Arneodo, J. Phys. (Paris) Lett. **41**, L243 (1980).

[9]J. E. Hirsch, B. A. Huberman, and D. J. Scalapino, Phys. Rev. A **25**, 519 (1982).

[10]H. J. Scholz, T. Yamada, H. Brand, and R. Graham, Phys. Lett. **82A**, 321 (1981).

[11]C. Meunier, M. N. Bussac, and G. Laval, Physica D **4**, 236 (1982).

[12]Y. Pomeau, J. C. Roux, A. Rossi, S. Bachelart, and C. Vidal, J. Phys. (Paris) Lett. **42**, L271 (1981).

[13]P. Bergé, M. Dubois, P. Manneville, and Y. Pomeau, J. Phys. (Paris) Lett. **41**, L344 (1980).

[14]J. Maurer and A. Libchaber, J. Phys. (Paris) Lett. **41**, L515 (1980).

[15]C. Jeffries and J. Perez, Phys. Rev. A **26**, 2117 (1982).

[16]M. Dubois, M. A. Rubio, and P. Bergé, Phys. Rev. Lett. **51**, 1446 (1983).

[17]F. Argoul and A. Arneodo, J. Mec. Theor. Appl. 241 (special issue, 1984).

[18]A. Arneodo, P. H. Coullet, E. A. Spiegel, and C. Tresser, Physica D **14**, 327 (1985).

[19]L. P. Shil'nikov, Sov. Math. Dokl. **6**, 163 (1965); Math. USSR-Sb. **6**, 427 (1968); **10**, 91 (1970).

[20]P. Gaspard and G. Nicolis, J. Stat. Phys. **31**, 499 (1983); P. Gaspard, Mémoire de Licence, University of Brussel, 1982 (unpublished).

[21]Such a rotational symmetry breaking indicates the existence of θ-dependent terms in the modulus equation in Eq. (3). This feature is corroborated by the detection of oscillations when plotting ρ_{n+1} vs ρ_n.

[22]P. Manneville, J. Phys. (Paris) **41**, 1235 (1980).

[23]A. Ben-Mizrachi, I. Procaccia, N. Rosenberg, A. Schmidt, and H. G. Schuster, Phys. Rev. A **31**, 1830 (1985).

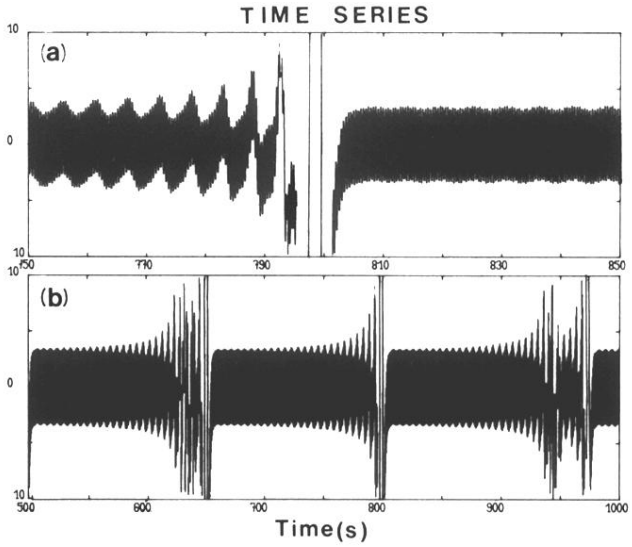

FIG. 2. Enlargements of the time series for $\mu = 1.25$. (a) and (b) differ in the dilatation rate of the time scale.